REPORT DOCUMENTATION PAGE

Form Approved
OMB No. 0704-0188

Public reporting burden for this collection of information is estimated to average 1 hour per response, including the time for reviewing instructions, searching existing data sources, gathering and maintaining the data needed, and completing and reviewing the collection of information. Send comments regarding this burden estimate or any other aspect of this collection of information, including suggestions for reducing this burden, to Washington Headquarters Services, Directorate for Information Operations and Reports, 1215 Jefferson Davis Highway, Suite 1204, Arlington, VA 22202-4302, and to the Office of Management and Budget, Paperwork Reduction Project (0704-0188), Washington, DC 20503.

1. AGENCY USE ONLY (Leave blank)	2. REPORT DATE	3. REPORT TYPE AND DATES COVERED
	27 Dec 1997	Performance Technical Report (SF 298)

4. TITLE AND SUBTITLE
NUMERICAL MODELING OF LASER BEAM PROPAGATION THROUGH NONLINEAR MEDIA

5. FUNDING NUMBERS
Contract or Grant Number: N00014-97-1-0936
R & T Project Number: 97 PR07274-00

6. AUTHOR(S)
Eric Van Stryland, David Hagan and Dmitri Kovsh

7. PERFORMING ORGANIZATION NAME(S) AND ADDRESS(ES)
CREOL, University of Central Florida
P.O. Box 162700
Orlando, FL 32816-2700

8. PERFORMING ORGANIZATION REPORT NUMBER

9. SPONSORING/MONITORING AGENCY NAME(S) AND ADDRESS(ES)
Office of Naval Research
Program Officer-Maribel R. Soto ONR 332
Ballston Center Tower One
800 North Quincy Street
Arlington, VA 22217-5660

10. SPONSORING/MONITORING AGENCY REPORT NUMBER

11. SUPPLEMENTARY NOTES

12a. DISTRIBUTION/AVAILABILITY STATEMENT
APPROVED FOR PUBLIC RELEASE

12b. DISTRIBUTION CODE
APPROVED FOR PUBLIC RELEASE

13. ABSTRACT *(Maximum 200 words)*

We are modeling the propagation of high intensity laser pulses through nonlinear optical materials including interactions of two-photon absorption, excited-state absorption and nonlinear refraction inlcuding thermal refraction. We have developed a preliminary code written in C++ applicable to Pentium-based PC's that is currently running and being tested against known results over a large range of input parameters. In particular, this code is being used to model optical limiting devices for sensor protection applications. While agreement is excellent for most nonlinearities at relatively low input energies, at high inputs, where transmittance values can drop to low levels, deviations are observed. It is thought that acoustic effects arising from thermal transients may be responsible. This is currently under investigation. We have recently developed an approximate solution for these photoacoustic nonlinearities that is computationally much faster than our previous code which was so computationally intensive that practical problems were prohibitive. This code is now being tested to verify its range of validity.

14. SUBJECT TERMS	15. NUMBER OF PAGES
Nonlinear optics, optical propagation	16. PRICE CODE

17. SECURITY CLASSIFICATION OF REPORT	18. SECURITY CLASSIFICATION OF THIS PAGE	19. SECURITY CLASSIFICATION OF ABSTRACT	20. LIMITATION OF ABSTRACT
UNCLASSIFIED	UNCLASSIFIED	UNCLASSIFIED	UL

NSN 7540-01-280-5500

19980121 113

Standard Form 298 (Rev. 2-89)
Prescribed by ANSI Std. Z39-18
298-102

Technical Report

Office of Naval Research (ONR)

Maribel Soto

Numerical modeling of the laser pulse propagation through the optical media with instantaneous and accumulative nonlinearities.

Eric Van Stryland: Principle Investigator

David Hagan: co-Principle Investigator

Dmitriy Kovsh: Graduate Student

Sidney Yang: Graduate Student

CREOL
University of Central Florida
Orlando, Florida 32816-2700

Abstract

We are modeling the propagation of high intensity laser pulses through nonlinear optical materials including interactions of two-photon absorption, excited-state absorption and nonlinear refraction including thermal refraction. We have developed a preliminary code written in C++ applicable to Pentium-based PC's that is currently running and being tested against known results over a large range of input parameters. In particular, this code is being used to model optical limiting devices for sensor protection applications. While agreement is excellent for most nonlinearities at relatively low input energies, at high inputs, where transmittance values can drop to low levels, deviations are observed. It is thought that acoustic effects arising from thermal transients may be responsible. This is currently under investigation. We have recently developed an approximate solution for these photoacoustic nonlinearities that is computationally much faster than our previous code which was so computationally intensive that practical problems were prohibitive. This code is now being tested to verify its range of validity.

The following lists the research results funded or partially funded by this ONR support along with a list of the personnel.

Book Chapter

"Z-scan Technique for Materials Characterization", Eric Van Stryland and M. Sheik-Bahae, in Materials Characterization and Optical Probe Techniques, Critical Reviews of Optical Science and Technology, Vol CR69, 501-524, SPIE 1997.

Conference Proceeding

"Reverse saturable absorption in polymethine dyes", S. Khodja, D. J. Hagan, J. Lim, O. V. Przhonska, S. Yang, J. Buckley and E. W. Van Stryland, Proc. SPIE-3146 (1997)

Invited Talks:

"Device Design and Materials Characterization for Passive Optical Limiters", Eric W. Van Stryland, David J. Hagan, Salah Khodja, Sidney Yang, D. Kovsh and Jinhong Lim, MRS Symposium: S, Materials for Optical Limiting II, Spring Meeting, San Francisco 1997.

"Z-scan Technique for Materials Characterization", Eric Van Stryland, Critical Review of Materials Characterization and Optical Probe Techniques for SPIE, San Diego, CA, 1997.

"Optical Limiting and the Potential Role of Organic Materials", Eric Van Stryland, Arthur Dogariu, Jin Hong Lim, David J. Hagan and Olga Przhonska, Organic Thin Films for Photonics Applications Meeting, Long Beach, CA, 1997.

"Optimization of optical limiting performance in strongly converging beam geometries" (Invited) D.J. Hagan, S. Khodja, S. Yang, D. Kovsh, P. Suedmeyer and E.W. Van Stryland, SPIE conf. on Nonlinear Optical Liquids, San Diego CA (July 1997)

Contributed Papers

"Optimization of solid-state passive optical limiters", S. Khodja, S. Yang, P. Suedmeyer, D. Kovsh, D. J. Hagan, and E. W. Van Stryland, CLEO'97, Baltimore, 1997.

Participants and their status

Eric Van Stryland: P. I.
David Hagan: co-P.I.
Salah Khodja: post-doc:
Dmitriy Kovsh: graduate student
Sidney Yang: graduate student

The following gives a more complete description of the most recent advances in this program

Prepared by Dmitriy Kovsh in collaboration with Sidney Yang who performed experiments.

Introduction

With the rapid success of computer technology the numerical modeling of pulsed laser beam propagation through nonlinear optical materials has become a powerful tool for investigating the interaction between light and matter. In addition, this modeling is now

progressing to the stage where nonlinear optical device design can potentially be performed numerically. A variety of algorithms have been developed and implemented in different areas of optical science including propagation in waveguide and fibers, the atmosphere, nonlinear optical materials and in laser cavity design. In our work performed under ONR sponsorship, we have focused on the numerical simulation of high-energy laser beam propagation in bulk nonlinear optical media. The main objective of our research is to develop a set of computer codes that will allow us to determine the influence of different nonlinear mechanisms and their coupling on the self-action of the propagating beam. One of the ultimate uses of this knowledge is to design passive optical limiting devices.

Taking advantage of the cylindrical symmetry of the common optical system (e.g. TEM_{00} laser mode or flat top beam) allows us to save computer time and memory by reducing the four dimensional (3D in space and 1D in time) problem to three dimensions (2D in space and 1D in time). Assuming that the pulse width is long enough and propagation distance short enough that we can ignore the dispersion of the material, the modeling of the beam self-action can be split into two separate tasks. (This is an excellent approximation for the systems under study.) The first of these tasks is the computing (and storing) of the spatial distribution of the nonlinear susceptibility within the sample for the particular moment in time. The second task is the CW propagation of each time slice through the material.

The first part of this report describes the numerical method we used to solve the paraxial wave equation in the nonlinear media. In the second part different nonlinear mechanisms are presented such as a Kerr-like index change, two-photon absorption, excited-state absorption and refraction as well as the refractive index change due to thermal lensing. At the end we show results of the numerical modeling of the laser pulse propagation through media having such nonlinearities. The comparison with the experimental data is given using a Z-scan setup and CCD camera outputs located at the image plane of the optical system.

Beam Propagation Algorithm

The propagation of light through the optical media can be described by the solution to the vector wave equation:

$$\nabla\times\nabla\times\vec{E}(\vec{r},t)+\frac{1}{c^2}\frac{\partial^2\vec{E}(\vec{r},t)}{\partial t^2}=-\mu_0\frac{\partial^2\vec{P}(\vec{r},t)}{\partial t^2}, \qquad (1.1)$$

where $\vec{E}(r_\perp,z,t)$ and $\vec{P}(r_\perp,z,t)$ are the electric field amplitude and the polarization. For the slow optical systems if the pulse width is long enough so the dispersion can be neglected this equation can be greatly simplified and rewritten in a scalar paraxial form:

$$2jk\frac{\partial\Psi(r_\perp,z,t)}{\partial z}=\nabla_\perp^2\Psi(r_\perp,z,t)+k_0^2\chi_{NL}(r_\perp,z,t)\Psi(r_\perp,z,t) \qquad (1.2)$$

and $E(r_\perp,z,t)=\Psi(r_\perp,z,t)e^{j\omega t-jkz}$. Here $\nabla_\perp^2$ and $r_\perp$ denote the transverse Laplace operator and spatial coordinate, while $\chi_{NL}(r_\perp,z,t)$ is the nonlinear susceptibility of the material (in

this formalism it also includes the linear absorption), which may, in general, consist of instantaneous and cumulative parts:

$$\chi_{NL}(r_\perp,z,t)=\chi_{NL}^{ins}(r_\perp,z)+\chi_{NL}^{acc}(r_\perp,z,t). \qquad (1.3)$$

Due to the fact that there is no explicit time dependence in Eq. (1.2) (although the field amplitude as well as the nonlinear susceptibility are in general functions of time), the modeling of the laser pulse propagation in the nonlinear media can be split into two separate numerical tasks. The first one is dividing the pulse into a number of time slices $\Psi(r_\perp,z,t_n)$ and propagating each slice as a CW beam. The second one is computing and storing the accumulative part of nonlinear susceptibility being induced by each slice $\chi_{NL}^{acc}(r_\perp,z,t_n)$. Therefore, the solution to the original time-dependent wave equation (1.2) becomes a CW propagation problem.

There is a variety of methods dealing with the paraxial wave equation in cylindrical coordinates. We use the second-order accuracy algorithm developed by Fleck et al. [1]. The transverse field distribution at the next step along z can be computed from the field distribution at the previous step using the formal solution to Eq. (1.2):

$$\Psi(r_\perp,z+\Delta z)=\exp\{-j\hat{S}(r_\perp,z)\Delta z\}\Psi(r_\perp,z), \quad (1.4)$$

with the propagation operator

$$\hat{S}(r_\perp,z)=\frac{1}{2k}\left(\frac{\partial^2}{\partial r^2}+\frac{1}{r}\frac{\partial}{\partial r}+k_0^2\chi_{NL}(r_\perp,z)\right) \qquad (1.5)$$

and taking the derivatives using 1D FFT. This algorithm, although not unitary, gives accurate results if the step Δz is chosen to be small enough (in our calculations this must be of the order of the wavelength).

It can be seen that this algorithm allows us to save computer memory by using only 2D arrays of data. The nonlinear susceptibility does not have to be saved with each step Δz. It is advisable to make this step Δz_{NL} in array of $\chi_{NL}^{acc}(r_\perp,z,t_n)$ larger (apparently it is convenient to make it to be equal to the multiple number of Δz), therefore, assuming that the nonlinearity does not change significantly within this distance we simply approximate it to be constant within Δz_{NL}. This allows us to reduce the size of the array $\chi_{NL}^{acc}(r_\perp,z)$. Also the chosen method for CW propagation has proven to be highly efficient, which allows us to model the propagation of the beam through a distance of tens or even hundreds of Rayleigh ranges, while the beam changes its size by several orders of magnitude. Figure 1 shows the results of a test of the accuracy of this method on the linear propagation of the Gaussian beam where an analytical solution is possible.

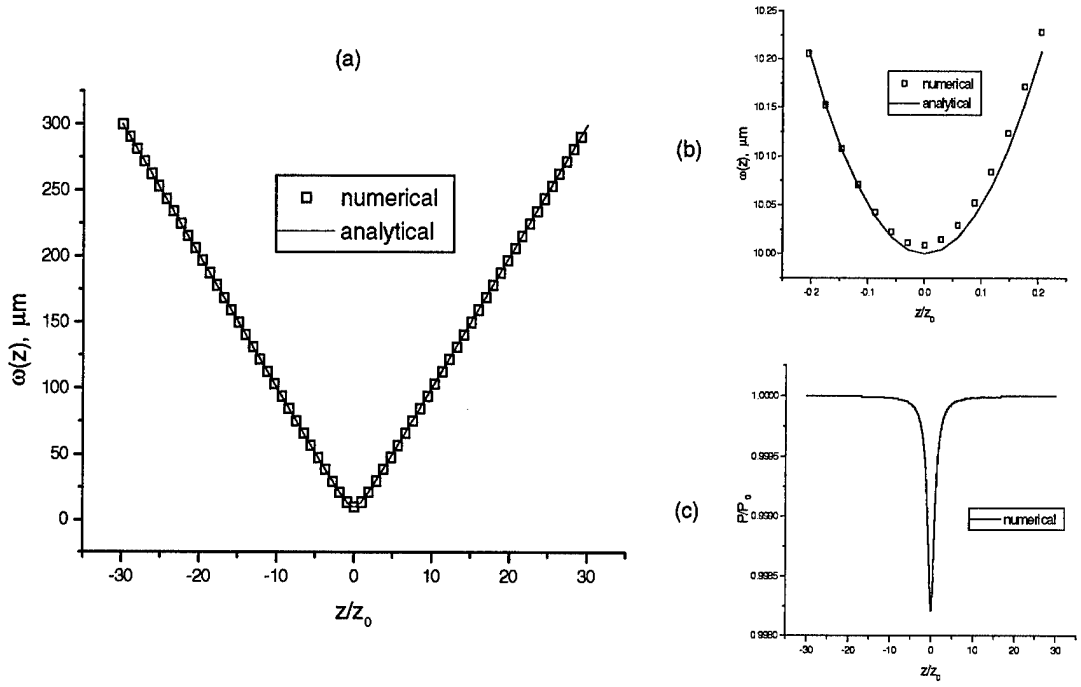

Fig. 1 Comparison of Gaussian beam size (a),(b) and power (c) calculated numerically and analytically. Maximum error occurs at the waist and is equal to 0.09% for the size (b) and 0.18% for the power (c).

Nonlinear Mechanisms

The nonlinear susceptibility as given in Eq. (1.5), is related to the nonlinear refractive index change and the absorption of the material as:

$$\mathrm{Re}\{\chi_{NL}^{ins}(\vec{r})\} = 2n_0\Delta n \quad (2.1)$$

$$\mathrm{Im}\{\chi_{NL}^{ins}(\vec{r})\} = -\frac{n_0}{k_0}\alpha\,,\ \alpha = \alpha_L + \alpha_{NL}$$

Here n_0 and k_0 are the linear index of refraction and the wave vector in vacuum, while α_L is the linear absorption coefficient and α_{NL} the nonlinear absorption coefficient of the material.

Instantaneous Nonlinearity

If the nonlinear response of the material has a characteristic time much shorter than the pulsewidth (for our purposes shorter than a few picoseconds), then we can consider it to be instantaneous and can be described by the first term of the nonlinear susceptibility Eq. (1.3). Typical examples of such nonlinearities are the bound-electronic nonlinear Kerr effect (nonlinear refractive index n_2) and two-photon absorption, 2PA (of 2PA coefficient β). The relations for these quantities are:

$$\Delta n = n_2 I(\vec{r}) \quad (2.2)$$

$$\alpha_{NL} = \beta I(\vec{r})\,. \quad (2.3)$$

Excited-State Nonlinearities

Excited-state absorption is a well-known process, which corresponds to absorption caused by a transition from an excited state to the next higher energy level. In order to have the excited state occupied it must be previously excited from the ground state. Therefore, excited-state processes follow linear absorption (or nonlinear absorption). Depending on whether the excited-state cross section of the material is smaller than that of the ground state or larger, we can distinguish saturable absorbers and reverse saturable absorbers (RSA). RSA was shown to be a very attractive nonlinearity for passive optical limiters (devices which are transparent for low energy light but "limits" its transmittance to high energy inputs) since the material becomes highly absorptive when the input fluence of the beam increases. Since this nonlinear effect accumulates in time as the integral of the irradiance with time (fluence) this nonlinearity is effective for longer pulses than are instantaneous nonlinearities. It has also been shown that several organic materials exhibit RSA properties in the visible region, including phthalocyanines, naphthalocyanines and their derivatives, and polymethine dyes. The energy level structure of those materials can be approximated by a five level model (see Figure 2), where the G-S1 transition represents the linear absorption and S1-S2, or T0-T1 – excited-state absorption. Time constants and cross section values have been experimentally investigated for TBP, SiNc, PbPc and several other materials.

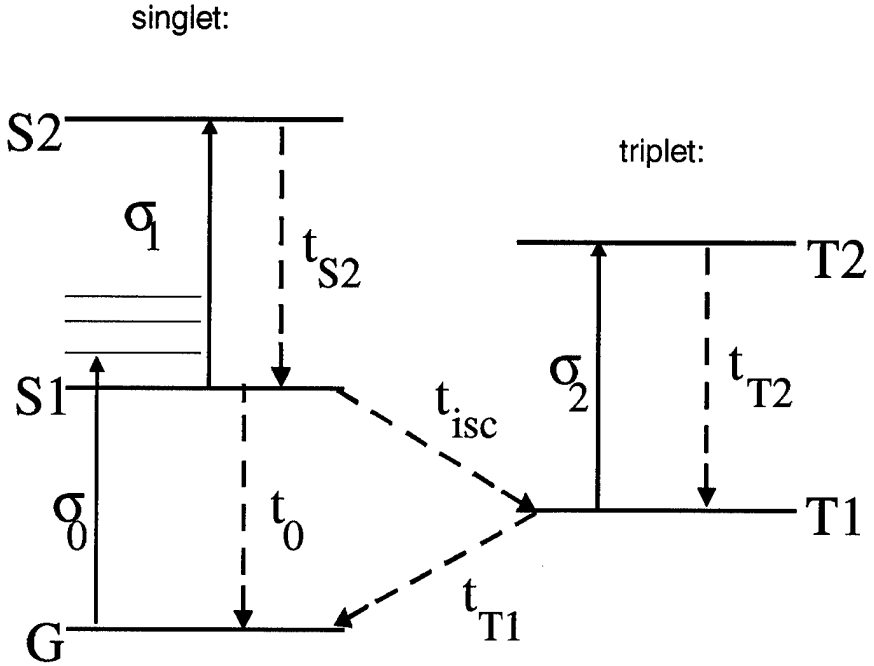

Fig. 2 Five-level system

The overall absorption of the system can be derived as a function of the populations of the levels:

$$\alpha = \sigma_0 N_G + \sigma_1 N_{S1} + \sigma_2 N_{T1}, \quad (2.4)$$

where $\sigma_1, \sigma_2 >> \sigma_0$, since those materials are reverse saturable absorbers. The dynamics of the five-level system can be described by a set of five rate equations that usually can be simplified for a particular time scale of the laser pulse, reducing the computation time. For nanosecond pulses, a good approximation is obtained by assuming the decay time of levels S2 and T1 are much smaller than the pulsewidth (usually τ_{S2} and τ_{T1} are of the order of a few picoseconds or less). This eliminates the need for tracking the populations of levels S2 and T1 since their populations remain near zero. Also if the decay time of first triplet level τ_{T0} is much longer than the pulsewidth, it can be taken as infinite. These simplifications result in:

$$\begin{aligned} \frac{dN_{S1}}{dt} &= \sigma_0 N_G \frac{I}{\hbar\omega} - \frac{N_{S1}}{\tau_{S1}} \\ \frac{dN_{T1}}{dt} &= \frac{N_{S1}}{\tau_{isc}} \\ N_G + N_{S1} + N_{T1} &= N_0 \end{aligned} \quad (2.5)$$

Here the overall lifetime of S1 is $1/\tau_{S1} = 1/\tau_0 + 1/\tau_{isc}$, where τ_{isc} is the intersystem crossing time which characterizes the dynamics of decay from the singlet manifold to the triplet manifold. The triplet yield is given by $\phi = \tau_{S1}/\tau_{isc}$ and N_0 is the total density of molecules (atoms or ions). If the laser pulse is in the 10's of picoseconds range, decay to the triplet manifold can be entirely ignored, since $\tau_{isc} >> \tau_p$ and thus the five-level system can be reduced to a three-level system which for the case of no saturation of the level S2, has an analytical solution.

Since the materials exhibit excited-state absorption, they show excited-state refraction as well – a consequence of causality giving Kramers-Kronig relations. However, the magnitude and sign of this nonlinear refraction has a different frequency dependence from the nonlinear absorption. This nonlinear refractive index change for several materials has been observed and mathematically can be represented by a refractive cross section proportional to the density of excited states:

$$\Delta n = \frac{\sigma_{S1,r} N_{S1} + \sigma_{T1,r} N_{T1}}{k}, \quad (2.6)$$

where $\sigma_{S1,r}$ and $\sigma_{T1,r}$ are refractive cross sections of the first singlet and triplet levels and k is the wave vector.

Thermal Effect

It was experimentally observed that a high-energy laser pulse, while passing through absorptive liquid media, induces temperature and density gradients that change the refractive index profile. This process is often called the thermal lensing effect, since the change in refractive index develops a negative lens inside the media. This phenomenon

has been rigorously studied both experimentally and theoretically. Moreover, for various time scales the thermal effect has different properties. For time scales longer than a few microseconds, thermal diffusion is the main source for the temperature gradient. Heating the material in this case can be described by the following equation:

$$\rho C_p \frac{\partial T}{\partial t} - \chi \nabla^2 T = \alpha I, \qquad (2.7)$$

where ρ is the density of the media, C_p is the specific heat at constant pressure, α - the absorption coefficient and χ - the thermal conductivity of the material. The refractive index change is, in general, a function of temperature and density changes inside the material:

$$\Delta n = \left(\frac{\partial n}{\partial \rho}\right)_T \Delta\rho + \left(\frac{\partial n}{\partial T}\right)_\rho \Delta T. \quad (2.8)$$

Therefore, Δn is linearly proportional to the temperature change if the density is constant, and the index of refraction changes due to thermal diffusion. However, for shorter times (the nanosecond time scale), density changes occur due to the acoustic wave generated by local heating and expansion of the liquid media. For picosecond pulses, the acoustic waves do not have time to develop, and therefore the density cannot change and the refractive index remains fixed except for other types of nonlinearities. Thermal refractive index changes in solid media also occur but are usually an order of magnitude smaller than in liquids and are often masked by the electrostrictive effect.

According to the derivation given in the Appendix, the index change induced by propagation of a nanosecond laser pulse through a liquid can be described by the following acoustic wave equation:

$$\nabla^2(\Delta n) - \frac{1}{C_S^2}\frac{\partial^2(\Delta n)}{\partial t^2} = -\frac{\gamma^e \beta}{2n}\nabla^2 T, \quad (2.9)$$

where C_S is the velocity of sound, β - the thermal expansion coefficient and γ^e - the electrostrictive coupling constant. For typical values of the sound velocity in liquids ($1 \div 2\times 10^3\, m/\mathrm{sec}$) if we have a few nanosecond long pulse focused to a spot size of 10 to 20 μm in diameter, the back part of the pulse is diffracted by the acoustic wave induced by the front part of the same pulse. To simplify the numerical modeling of the photoacoustic effect we can parameterize the index change close to the propagation axis by the following expression (see the Appendix):

$$\Delta n \cong \left(\frac{\partial n}{\partial T}\right)_0 \Delta T, \text{ where } \left(\frac{\partial n}{\partial T}\right)_0 = \frac{\gamma^e \beta}{2n}. \quad (2.10)$$

With such an approximation we can significantly reduce the computational time required to numerically solve the acoustic wave equation for each time slice of the pulse. In fact, there are a number of experimental results in the literature where this thermo-optic coefficient was calculated in this approximation for different liquids. One has to be careful using the approximation Eq. (2.20) and the experimental data for the effective Δn published in the literature. Equations (2.10) assumes that the thermal lens is being induced instantaneously and ignores the small index disturbances on the sides of the

pulse which are due to the acoustic wave propagation. Figure 4 shows the comparison between the refractive index change (nonlinear phase shift) obtained by solving the full acoustic wave equation (2.9) and the one obtained using the relation (2.10). This approximation is only valid when the characteristic length of the acoustic wave $C_s\tau_p$ is larger than the beam size. If the beam size is too big the acoustic wave does not have enough time to grow within the pulse (this case is presented in the Figure 6). Thus, the approximation (2.10) will show the larger index change (stronger nonlinear lens is being introduced as could be seen in the Figure 7). Also if this approximation were used to analyze the experimental data (for example Z-scan curves), the value of the thermo-optic coefficient $(\partial n/\partial t)$ could be incorrect.

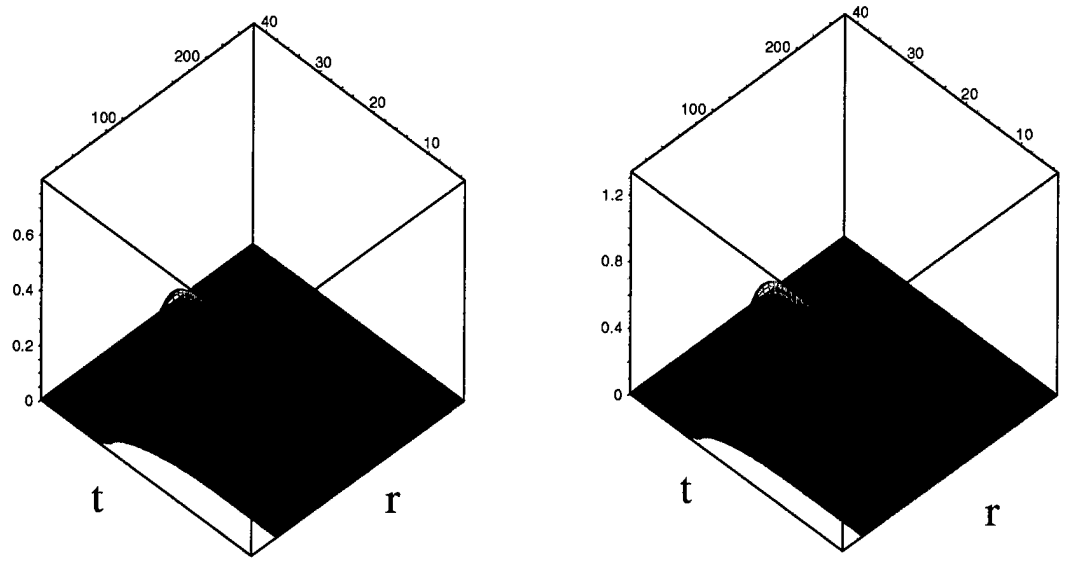

Fig. 3 Temperature change ΔT(r,t) due to thermal effect. Nigrosine in water.
left: Ein = 2 μJ, $\omega = 8$ μm, $\tau = 10$ *ns* (FWHM). right: Ein = 30 μJ, $\omega = 30$ μm, $\tau = 10$ *ns* (FWHM).

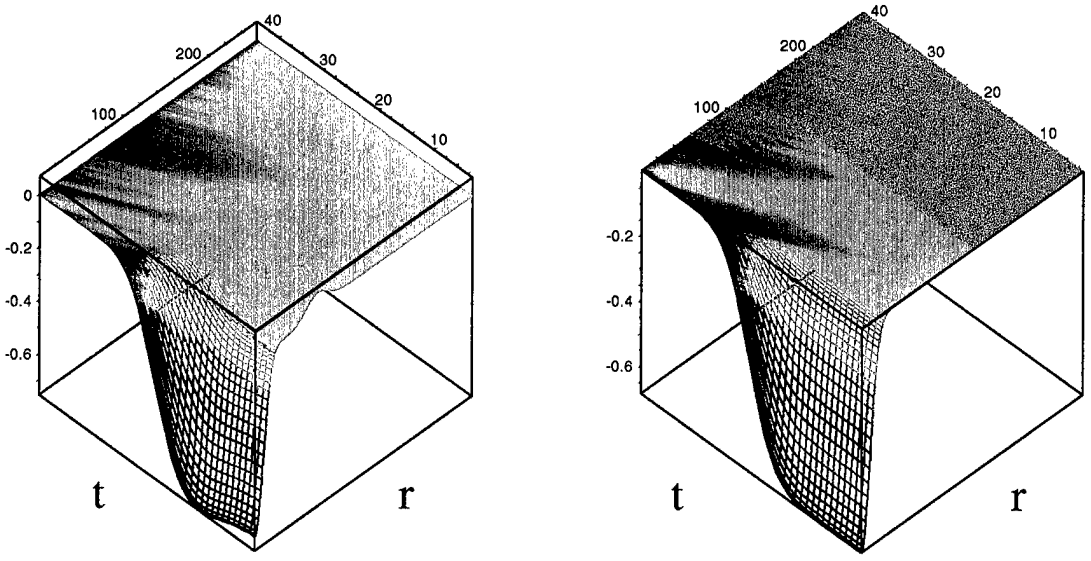

Fig. 4 nonlinear phase shift ΔΦ(r,t) due to photo-acoustic effect (left) and thermal lensing approximation (right). Nigrosine in water. Ein = 2 μJ, $\omega = 8$ μm, $\tau = 10$ *ns* (FWHM).

As was mentioned above, heating of the material is caused by absorption of the laser beam energy, however, the mechanisms of such absorption can vary. We first model the thermal lensing and photoacoustic effects induced by linear absorption. Figures 3-7 show the temperature change distribution as well as the introduced nonlinear phase shift (proportional to the refractive index change) and far-field fluence distribution calculated while propagating a 20 nsec FWHM pulse through a water solution of nigrosine. Nigrosine is chosen since it shows very little nonlinear response other than thermal refraction from linear absorption for nanosecond inputs. The comparison of the results with ones obtained with the approximation Eq. (2.10) is also presented.

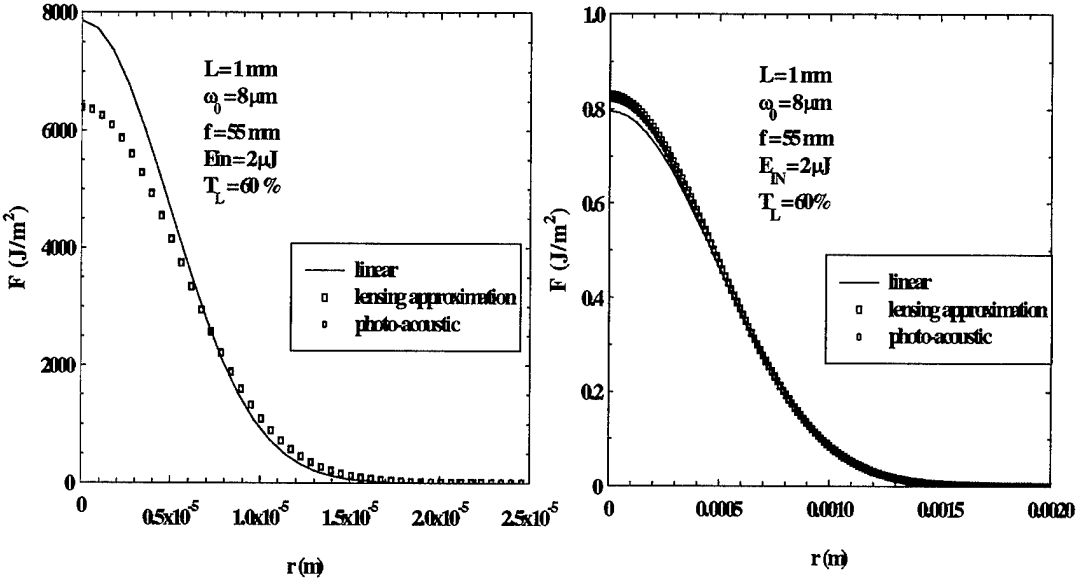

Fig. 5 Fluence distribution after the sample (left) and in the far field (right) if nonlinear refractive index change was computed by solving the acoustic wave equation and with lensing approximation ("linear" corresponds to the case with no nonlinearity)

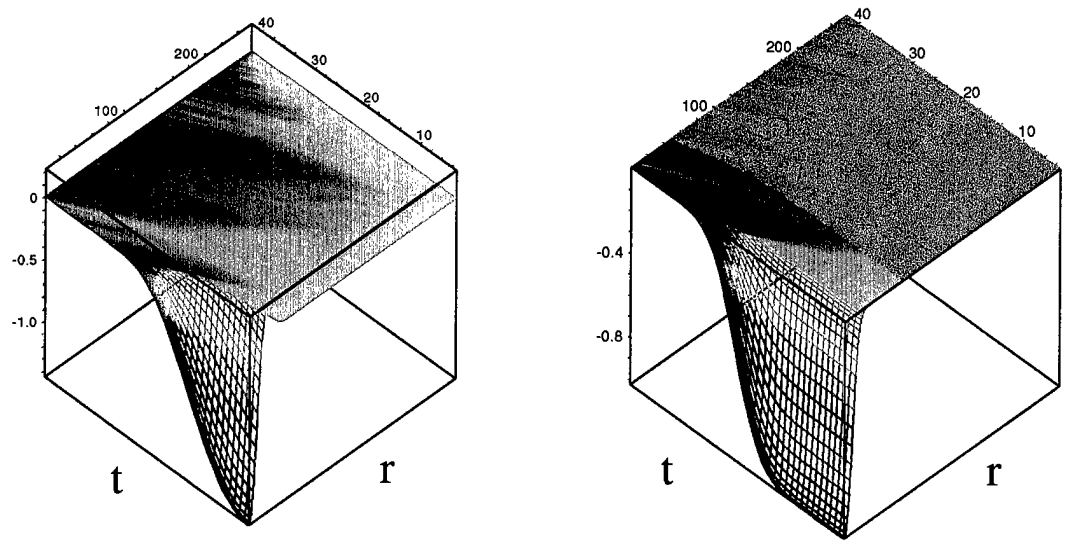

Fig. 6 nonlinear phase shift $\Delta\Phi(r,t)$ due to photo-acoustic effect (left) and thermal lensing approximation (right). Nigrosine in water. Ein = 30 μJ, $\omega = 30$ μm, $\tau = 10$ ns (FWHM).

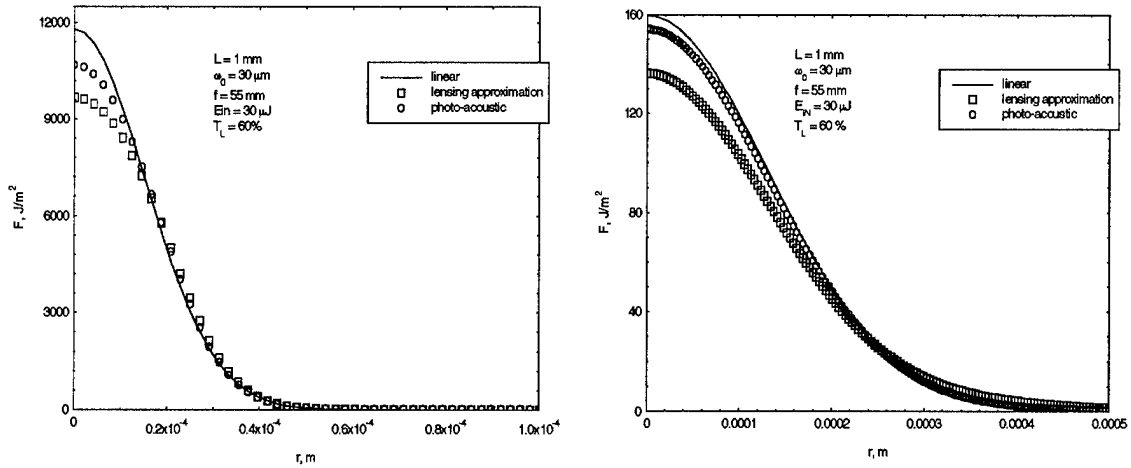

Figure 7. Fluence distribution at the exit plane of the sample (left) and in the far field (right) if nonlinear refractive index changes are computed by solving the acoustic wave equation and with the lensing approximation ("linear" corresponds to the case with no nonlinearity).

A comparison of the predictions of this model with the results of a Z-scan on the solution of nigrosine is shown in Fig. 8. These curves show excellent agreement.

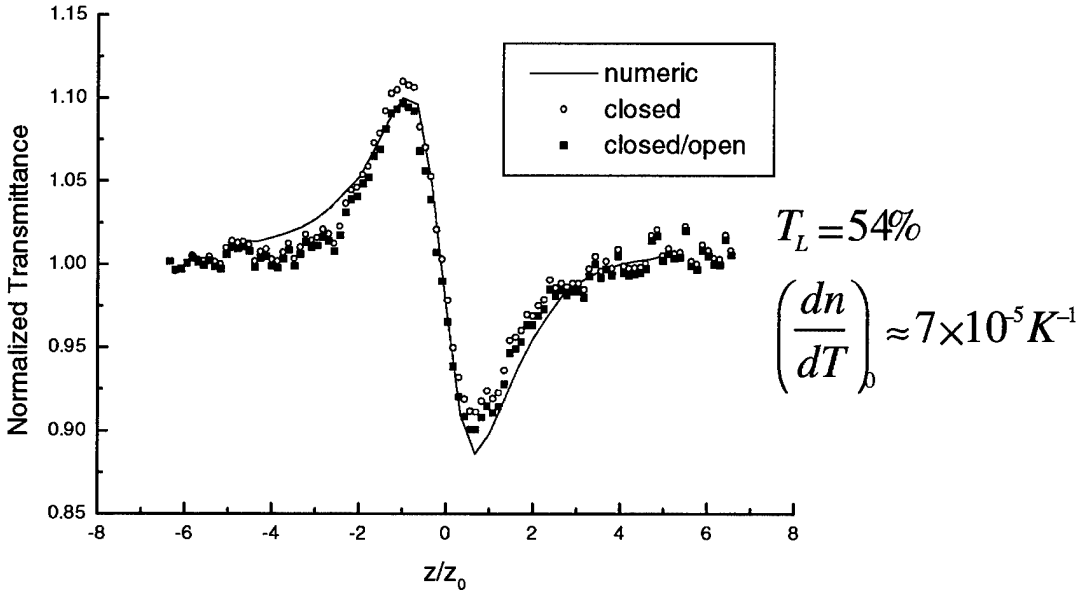

Figure 8. A comparison of the experimental Z-scan (using a Gaussian input beam) performed on a solution of nigrosine in water for 20 nanosecond (FWHM) 532 *nm* pulses at an energy of 0.4 μJ focused to the 6 μm waist.

If we consider the source of the thermal effect to be RSA, we can evaluate the significance of this effect by running the propagation code including RSA only and including both RSA and the photoacoustic effect together.

Flat-Top Beam Analysis

We have also performed experiments and analysis of so-called flat-top beams. We experimentally produce these by expanding an initially Gaussian bean and sending it through a finite aperture which clips the beam to approximate a flat-top beam. Figure 9 shows a comparison of the calculated radial energy distribution with the experimental distribution for nigrosine with the detector located at the image plane of the flat-top beam. The sample is located at the position corresponding to the minimum of the Z-scan curve (Figure 10).

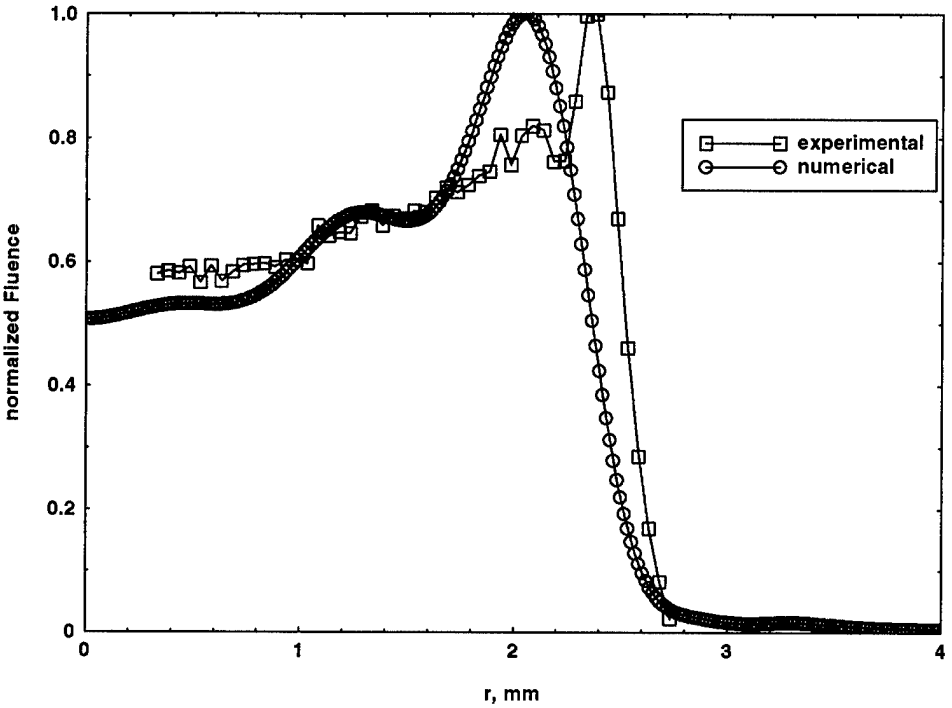

Figure 9. Normalized fluence distribution in the image plane. Sample is located at the point which corresponds to the minimum of the Z-scan curve (see the next Figure).

Figure 10 also shows the comparison of the experimental Z-scan curve with the numerical one.

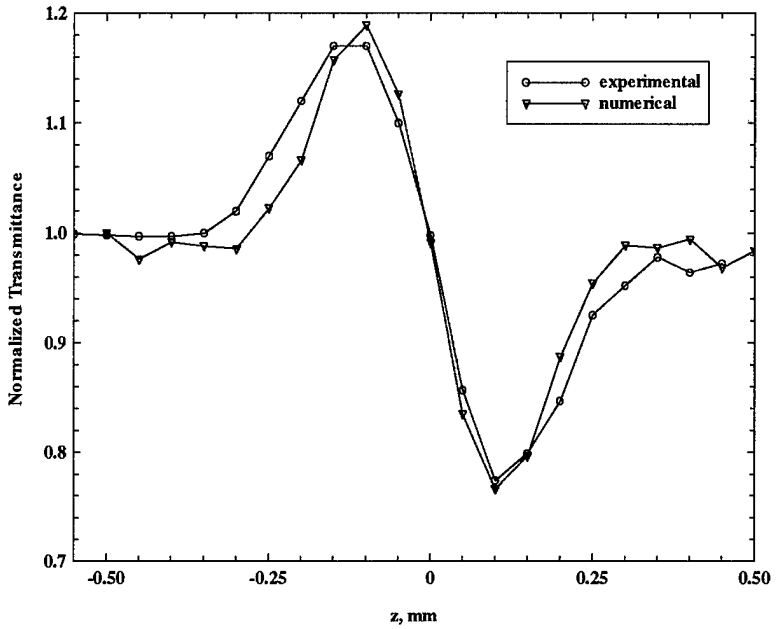

Figure 10. Z-scan using a flat-top beam for nigrosine in water. Experimental (circles), numerical (triangles).

Limiting

We have also compared the results of calculation using this model to the results of limiting experiments. Figure 10 shows the design of a 3-element (liquid filled cuvettes) optical limiter using solutions of zinc-tetrabenzporphyrine (TBP obtained from Natick). The comparison of data with experiment is shown in Fig. 11. The theory matches experiment well except for very large input energies where significant differences are seen. These differences may indicate that the thermal lensing approximation is breaking down and that it may be necessary to solve the full acoustic wave equation at high inputs.

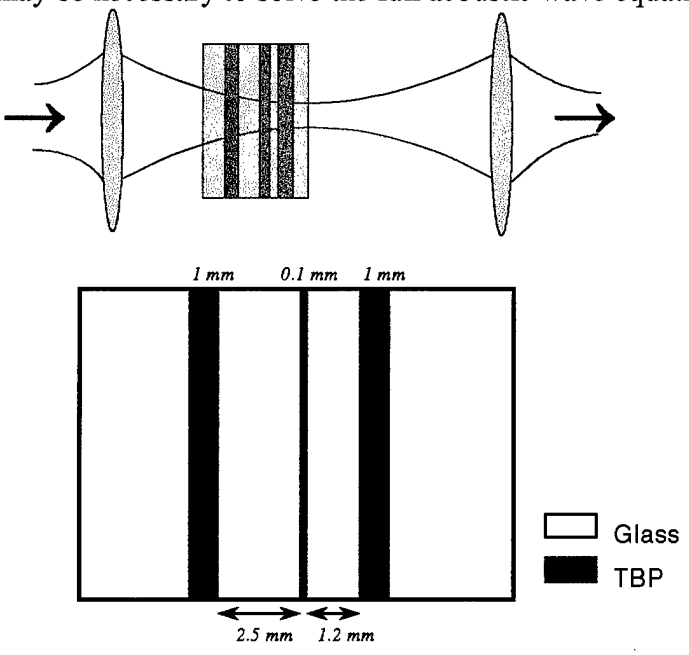

Figure 10. Schematic of the design of the 3-element TBP limiter.

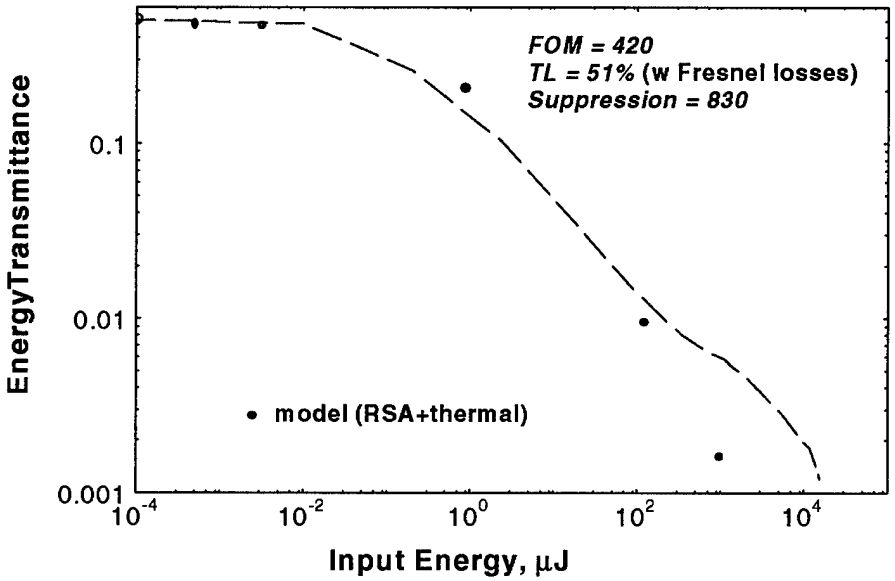

Figure 11. Comparison of the calculated (circles) energy transmittance for the 3-element tandem limiter to experiment (dashed line).

Conclusion

We have developed computationally efficient computer codes for modeling the propagation of high irradiance laser pulses through thick (several Rayleigh ranges) nonlinear optical materials including several nonlinear mechanisms relevant to optical limiting. Besides the inclusion of both ultrafast nonlinear absorption and refraction, we have included the effects of excited states on both the absorption and refraction. These nonlinearities accumulate with time within a laser pulse. Computationally this requires the code to remember previous parts of the laser pulse. We have also included the effects of thermal lensing with the added complication of the acoustic waves generated by linear and nonlinear absorption. This requires simultaneous solutions to two wave equations and is extremely computationally intensive. In order to produce a more time efficient code we have studied the region of validity of an approximate solution to the acoustic wave equation. Comparisons between the output of this code to experiments are still ongoing. In addition other numerical methods and approximations are being studied.

Appendix

When the liquid or gas media absorbs energy from the laser beam, it results in changes of density, temperature, pressure and fluid velocity. The general form of the equations describing such changes is the following:

$$\frac{\partial \rho'}{\partial t} + \rho \nabla \cdot \mathbf{v}' = 0$$

$$\rho \frac{\partial \mathbf{v}'}{\partial t} + \nabla p' = \nabla F \qquad , \qquad \text{(A.1)}$$

$$\rho c_v \frac{\partial T'}{\partial t} - \left(\frac{p}{\rho}\right)\frac{\partial \rho'}{\partial t} = Q$$

where ρ is the density, p pressure, T - the temperature and v - the fluid velocity of the media. The quantities without the prime are undisturbed properties of the material, while the ones with the prime characterize the changes due to the absorption of laser light energy. c_v is the specific heat at a constant pressure. We can now write

$$Q(r,t) = \left(\frac{\partial p}{\partial t}\right)_\rho \frac{\alpha I(r,t)}{\rho c_v} \qquad \text{(A.2)}$$

which is responsible for the heating effect induced by the laser beam with intensity $I(r,t)$ and

$$F(r,t) = \rho\left(\frac{\partial \varepsilon}{\partial \rho}\right)_T \frac{I(r,t)}{c_S} \qquad \text{(A.3)}$$

for the electrostictive effect. c_S is the isotropic sound speed $c_s = \sqrt{(\partial p/\partial \rho)_S}$. Equations in (A.1) are linearized with respect to small changes in media characteristics (variables with prime) and can be viewed as conservation of mass, momentum and energy respectively. In literature references an alternative form of the starting equations was chosen, however the results obtained are basically the same.

If a liquid media is under consideration, the electrostrictive effect can usually be neglected and the equation for the density change will be:

$$\left(\frac{\partial}{\partial t}\right)\left[\left(\frac{\partial^2 \rho'}{\partial t^2}\right) - c_S^2 \nabla^2 \rho'\right] = \nabla^2 Q . \qquad \text{(A.4)}$$

By integrating the last equation we obtain the acoustic wave equation for the density change inside the media:

$$\left(\frac{\partial^2 \rho'}{\partial t^2}\right) - c_S^2 \nabla^2 \rho' = \int_{-\infty}^{t} \nabla^2 Q(r,t')dt' . \quad \text{(A.5)}$$

In a liquid media the refractive index change is given by

$$\Delta n = \left(\frac{\partial n}{\partial \rho}\right)_T \Delta\rho + \left(\frac{\partial n}{\partial T}\right)_\rho \Delta T = \frac{\gamma^e}{2n\rho}\Delta\rho + \left(\frac{\partial n}{\partial T}\right)_\rho \Delta T , \qquad \text{(A.6)}$$

where γ^e is the electrostrictive coupling constant and

$$\gamma^e = \rho\left(\frac{\partial n^2}{\partial \rho}\right)_T = \frac{(n^2-1)(n^2+2)}{3} . \qquad \text{(A.7)}$$

For liquid media, the index is usually much more sensitive to density changes, therefore contributions due to temperature variations can be neglected (second term in (A.6) is zero). Using this fact and two well-known relations:

$$(\partial p/\partial T)_\rho = \rho\beta(\partial p/\partial T)_T, \quad \frac{(\partial p/\partial \rho)_T}{c_v} = \frac{(\partial p/\partial \rho)_S}{c_p} \qquad \text{(A.8)}$$

we can write down the wave equation for the refractive index change:

$$\frac{\partial^2(\Delta n)}{\partial t^2} - c_S^2\nabla^2(\Delta n) = \frac{\gamma^e}{2n\rho}\frac{\beta c_S^2}{c_p}\int_{-\infty}^{t}\nabla^2(\alpha I(r,t'))dt'. \qquad \text{(A.9)}$$

The source factor in the last equation can be expressed in terms of the temperature change. The general heat balance equation

$$\rho c_p\frac{\partial T}{\partial t} - \chi\nabla^2 T = \alpha I, \qquad \text{(A.10)}$$

where χ is the thermal conductivity of the material, can be integrated for nanosecond pulses (ignoring temperature diffusion on this time scale) to yield

$$T(r,t) = \frac{1}{\rho\ c_p}\int_{-\infty}^{t}\alpha I(r,t')dt'. \text{ (A.11)}$$

Combining (A.9) and (A.11) we can obtain the final form of the acoustic wave equation for refractive index change:

$$\frac{\partial^2(\Delta n)}{\partial\ t^2} - c_S^2\nabla^2(\Delta n) = \frac{\gamma^e\beta\ \ c_S^2}{2n}\nabla^2 T(r,t'). \qquad \text{(A.12)}$$

The fractional index change can be parameterized in the paraxial approximation (close to the laser beam axis) as [2]:

$$\frac{\Delta n(r,t)}{n} = \left[1 - \frac{r^2}{2}\frac{\nabla^2\rho'(r=0,t)}{\rho} + \ldots\right]\left(\frac{\partial n}{\partial \rho}\right)_T\frac{\rho'(r=0,t)}{n} \qquad \text{(A.13)}$$

and if only the first term in the expansion (A.13) is taken into account

$$\Delta n = \left(\frac{\partial n}{\partial T}\right)_0\Delta T, \text{ where } \left(\frac{\partial n}{\partial T}\right)_0 = \frac{\gamma^e\beta}{2n}. \qquad \text{(A.14)}$$

The expression (A.14) is a commonly used approximation called the thermal lensing effect which is usually used for longer time scales $c_S t/a > 1$ (microseconds), where a is the radius of the beam. The coefficient in the last equation is called the thermo-optic coefficient and it has been measured for some organic solvents. Equation (A.12) can also be obtained from the derivation given in Ref. [3] if the definition (A.7) is used.

References

1. M. D. Feit, J. A. Fleck, Jr., "Simple Method for Solving Propagation Problems in Cylindrical Geometry with Fast Fourier Transforms", Optics Letters, Vol. 14, No. 13, July 1, 1989
2. P. R. Longaker, M. M. Litvak, "Perturbation of the refractive Index of Absorbing Media by a Pulsed Laser Beam", Journal of applied Physics, 40, 1969, 4033
3. TieJun Xia, "Modeling and Experimental Studies of Nonlinear Optical Self-Action", Ph.D. thesis